Annealing influences on phosphorus-ion-implanted vicinal Si(111) studied by reflective second-harmonic generation

Kuang Yao Lo* and Yi Jen Huang

Department of Applied Physics, National Chia Yi University, Chia Yi, Taiwan 600, Republic of China
and Institute of Optoelectronics and Solid State Electronics, National Chia Yi University, Chia Yi, Taiwan 600, Republic of China

(Received 21 August 2006; published 3 July 2007)

Annealing effects on the implanted vicinal Si(111) were analyzed by reflective second-harmonic generation (RSHG). The phenomena of impurity diffusion and precipitation were observed through the anisotropic contribution of the C_{3V} component in the RSHG rotational anisotropy experiments for a series of rapid thermal annealing (RTA) times. The surface reconstruction of the implanted vicinal Si(111) was clearly observed due to the contribution of the C_{1V} symmetry which is raised from the step structure on the vicinal surface. The enhanced value of the C_{1V} component originates because P atoms participate in the surface reconstruction. The phase difference between the C_{3V} and C_{1V} components has large variations at lower RTA temperature because the reconstruction situation near the surface was not completed until the RTA time of 30 s and was influenced by the precipitation of P atoms. With the assistance of step structure on vicinal Si(111), the reconstruction of the implanted Si(111) reveals more physical information.

DOI: 10.1103/PhysRevB.76.035302 PACS number(s): 78.20.−e, 42.65.−k, 61.72.Tt

I. INTRODUCTION

Optically reflected second-harmonic generation (RSHG) has proven to be a sensitive tool for obtaining information on the structural and electronic properties of metal and semiconductor surfaces.[1,2] The symmetrical group of the silicon surface differs from that of the silicon bulk, which is a centrosymmetrical media.[3] RSHG is forbidden within the electric-dipole approximation in centrosymmetrical media and only allowed on the surface and interfaces, where the bulk symmetry is broken. Therefore, the RSHG signal is very strongly influenced by the surface layer of these materials, where the reduced symmetry enables the SHG process. Anisotropic contributions to RSHG intensity have been used for studies of the phenomenological theory and analysis from Si.[1,4] SHG rotational anisotropy (RA-SHG) is indeed highly sensitive to the microscopic structure and symmetrical properties of the silicon interface structure.[5]

To obtain the higher performance of very large scale integration, it is necessary to deeply understand the mechanism of thin film growth. One of the chief issues the silicon device industry faces for miniaturization is the production of ultrashallow doped layers,[6] since the formation of ultrashallow layers is important for the fabrication of nanosemiconductor devices. In particular, variations in the interface of the ultrashallow layer during the thermal process will influence the device performance.[7] A high degree of reproducibility and control of dopant purity, dosage, and spatial distribution for the requirement in the ultrashallow doped layers can be achieved by low-energy ion implantation techniques and rapid thermal annealing (RTA) processes. RTA technology is an efficient technique to remove the ion implantation damage, activate dopant impurities, and produce a surface with crystal quality and sheet resistance equal to or greater than those obtained by conventional furnace annealing, but with the advantage of reduced impurity redistribution.[8]

The results of the low-energy implanted silicon dealt with the RTA process have been successfully diagnosed by the RA-SHG method,[9] and theoretical analyses have been presented to explain the actual phenomena in the RTA process.[10] This nondestructive method presented an illustration of the recrystallization degree in the shallow region that was not explained by traditional x-ray diffraction. Our previous results showed that the RTA temperature is a key factor in recrystallizing the dosed range and diffusing the impurities within the expected range. After a suitable RTA process, the destroyed region of Si is recrystallized and implanted impurities enter the Si sites in the pattern of a well-ordered sublattice with polar bond behavior. Govorkov *et al.*[11] pointed out that the inhomogeneous strain-induced contribution to the second-order nonlinear susceptibility tensor would have the same nonvanishing components as the surface-dipole nonlinear susceptibility tensor. The residual electrical dipoles are formed along the surface symmetry during the RTA process, since implanted impurities enter the Si sites with enough activation energy. These are additional SHG sources from the implanted silicon.[10] Accordingly, Lo presented the potential of identifying the recrystallized condition during the RTA treatment by analyzing RSHG patterns.[10] However, the analysis results of the RSHG method are integrated over the surface region, which is limited by the penetration depth of the incident light. Thus, further formations on the top surface layers of implanted silicon would be hidden in the bulklike surface region layer.

Recently, vicinal Si(111), which is cut with a small offset angle towards the $[11\bar{2}]$ direction, was used in the SHG studies for the surface adsorption and buried interface since vicinal Si(111) surface reflects a onefold symmetry originating from the surface steps in the $[11\bar{2}]$ direction.[11–13] Except for the contribution of threefold symmetry (C_{3V}) from the (111) terraces, the appearance of steps on the vicinal Si(111) surface gives a strong effect in observing RA-SHG and this result is consistent with the regular step structure having C_{1V} symmetry. RA-SHG studies of Si-O bondings on vicinal Si(111) and H-atom termination have suggested that the onefold contribution to the SHG signal comes primarily from Si atoms at or in the immediate vicinity of the surface steps.[12–14] These studies revealed that the step structures on a

 ©2007 The American Physical Society

vicinal silicon surface give a C_{1V} symmetry contribution to the RSHG intensity, which is dependent on Si-O bonding arrangements on the step.[15]

In view of the indistinguishable RSHG contribution from both bulk and surface of silicon,[16] the step structures on the vicinal Si surface can help analyze RSHG intensity generated from surface components. The degree of the surface reconstruction could be diagnosed by examining the variation in the RSHG intensity from the implanted vicinal Si. Therefore, the use of dopant implantation on vicinal Si surface and proper RTA treatment on it are effective to reach the purpose of the surface analysis through RSHG measurements. In this paper, we used the phosphorus (P)-ion-implanted vicinal Si(111) in a series of RA-SHG studies to exhibit the variation in the surface layer during the RTA process. The phenomena of the recrystallization, impurity diffusion, and thermal relaxation in the surface layer of the implanted silicon would be obtained by analyzing the interference of a step-induced C_{1V} symmetry with an underlying C_{3V} symmetry of (111) terraces. Using secondary ion mass spectroscopy (SIMS) and transmitted electron microscopy (TEM), the recrystallization, the dopant diffusion, and the precipitation phenomena are examined by analyzing the RA-SHG results. This work shows the potential of the RSHG technique for analyzing the surface reconstruction during RTA treatment.

II. THEORY

The main source of the effective surface polarization $P^s_{eff}(2\omega)$ from the implanted Si(111) is acquired by integrating the effective radiated layer. The nonlinear optical sources from this interfacial layer are the surface-dipole sheet $[\chi^{(2)}_s]$, the bulk electric dipole $[\chi^{(2)}_D]$, and the bulk electric quadrupole $[\chi^{(2)}_Q]$. For the vicinal Si(111) surface, $\chi^{(2)}_s$ is not only contributed from the C_{3V} symmetry of the Si(111) terraces but also from the C_{1V} symmetry of the steps. The net dipole amount of the Si-O bonds $[\chi^{(2)}_{step}]$ on the steps also gives a contribution to the RSHG field.[11,12] For intrinsic silicon with inversion symmetry, the bulk dipole term $[\chi^{(2)}_D]$ is zero. In the low-energy ion implantation process, the implanted atoms destroy the silicon lattice and the amorphous layer is formed at the near-surface region. After a proper RTA process, the amorphous region of the Si(111) surface will be recrystallized and the weak polar bond of Si-P, which is treated as the residual electrical dipole due to implant ions entering the silicon site, is formed. The weak polar bond of Si-P is calculated by the bond orbital approach from previous research.[10] The residual electrical dipole term exists in the implanted Si layer, and its symmetry is similar to that of the surface of silicon.[11] Therefore, the effective surface polarization $P^s_{eff}(2\omega)$ of the implanted vicinal Si(111) contains the residual electrical dipole, the electric quadrupole which existed in the silicon substrate, and the net dipole amount of the Si-O bonds on the steps.

The enhanced SHG intensity from the implanted silicon is clearly explained and estimated by integrating the residual second-order susceptibility over the effective region, which includes the consideration of the absorption, the active degree, and the dopant distribution.[10] For the implanted vicinal Si(111), the nonlinear susceptibility of the step contribution $[\chi^{(2)}_{step}]$ could be added into the total RSHG intensity, which is modified from Ref. 10 and expressed as

$$I^{(2)}_{ijk}\alpha\left\{\int \chi^{(2),P}_{ijk} D_T(z)\exp[-\alpha(2\hbar\omega,z)z]\exp[-2\alpha(\hbar\omega,z)z]dz + |k|\alpha^{-1}(2\hbar\omega,z)\chi^{Q}_{eff} + \chi^{(2)}_{step}\right\}^2, \quad (1)$$

where $\chi^{(2),P}_{ijk}$ is the residual electrical dipole that is formed with Si and P atoms, $D_T(z)$ is the dopant distribution function at RTA temperature of T, k is the wave vector of incident light, and χ^{Q}_{eff} is the electric quadrupole of silicon substrate, which is equal to 5×10^{-13} esu for undoped silicon at $\lambda=1.064$ μm.[17] Furthermore, $\alpha(\hbar\omega,z)$ and $\alpha(2\hbar\omega,z)$ are the optical absorption coefficients for the fundamental light and second-harmonic light, respectively. There is a substantial increase in the optical absorption coefficient for P-doped sili-

TABLE I. The parameter amplitudes and the phase angle from differently treated implanted vicinal Si(111) surfaces obtained from the SS-SHG results and the absorption coefficients of second-harmonic light for these samples.

Sample	a_3	a_1	$a_3/a_{3,\mathrm{Si}}$	$a_1/a_{1,\mathrm{Si}}$	Ψ_1 (deg)	α (532 nm) (10^5 cm^{-1})
Si(111)	0.82	0.34	1.00	1.00	75	0.485
No RTA	0.56	0.30	0.68	0.87	70	1.928
850 °C 10 s	1.67	0.36	2.03	1.04	40	1.106
850 °C 20 s	0.89	0.43	1.08	1.25	42	1.071
850 °C 30 s	0.59	0.50	0.71	1.45	135	1.306
850 °C 40 s	0.46	0.51	0.56	1.48	140	1.337
900 °C 10 s	1.18	0.50	1.43	1.44	48	0.912
900 °C 20 s	0.89	0.53	1.08	1.55	55	1.060
900 °C 30 s	0.70	0.53	0.85	1.55	56	0.957
900 °C 40 s	0.61	0.50	0.74	1.44	58	1.142

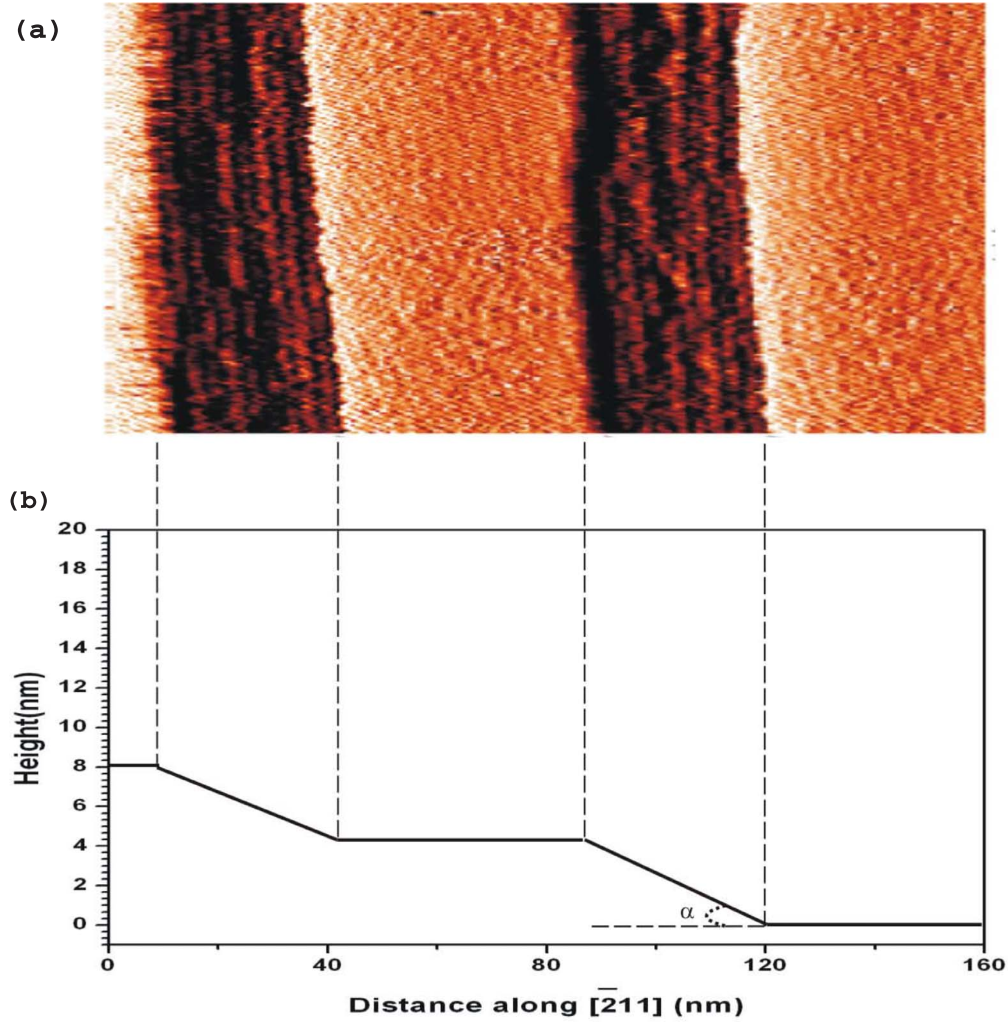

FIG. 1. (Color online) (a) STM image of vicinal Si(111) surface with bunched steps. (b) Line scan across the steps.

con, and the relationship between the absorption coefficient and the doping concentration can be empirically obtained.[17,18] The absorption coefficients of second-harmonic light for these samples were obtained from the Kramers-Kronig relation in analyzing the reflectance spectrum and are listed in Table I.

In the ion implantation process, the degree of deformation depends on the distance from the surface in a direction along the surface normal. The symmetry near the surface region would be violated along the normal direction. The lattice deformation under the uniaxial stress of Si(111) does not change the Si surface structure of C_{3V} symmetry.[11] The non-vanishing components of the second-order nonlinear optical susceptibility of the strained lattice are the same as those of the Si(111) surface.

The s-polarized SHG intensity for an s-polarized fundamental field, $I_{s,s}(2\omega)$, is most sensitive to the surface symmetry since this polarization combines anisotropic nonlinear susceptibility tensor elements, and the RA-SHG result of $I_{s,s}(2\omega)$ is referred to as SS-SHG for the convenience of the following discussion.[5] Thus, for the case of implanted vicinal Si(111) surface, $I_{s,s}(2\omega)$ is adopted to analyze the results and expressed as[19]

$$I_{S,S}(2\omega) = |a_1 e^{i\psi_1} \sin(\varphi) + a_3 \sin(3\varphi)|^2, \tag{2}$$

where the rotation angle φ is defined as the angle between the plane of incidence and the projection of the crystallographic [001] axis on the surface and a_3 is contributed from the residual electrical dipole $[\chi_{ijk}^{(2),P}]$ and bulk quadrupole $[\chi_{eff}^{Q}]$ and belongs to the C_{3V} symmetry. The contributions of a_1 originate from the step-induced dipoles $[\chi_{step}^{(2)}]$ in the vicinal Si(111) and belong to the C_{1V} symmetry. The phase difference ψ_1 between the a_1 and a_3 components has a strong dependence on the annealing condition and is correlated to the density of interface traps.[12] With assistance from the vicinal surface, more information on the implanted surface structure would be revealed by analyzing the above parameters in the SS-SHG experiments.

III. EXPERIMENTS

The vicinal Si(111) substrates were Czochralski p-type silicon wafers (10–20 Ω cm, B dopant). A scanning tunneling microscope (STM) experiment was made under the condition of a tunneling current of 0.8 nA and a sample bias of −2 V. The surface structure morphology of the silicon is

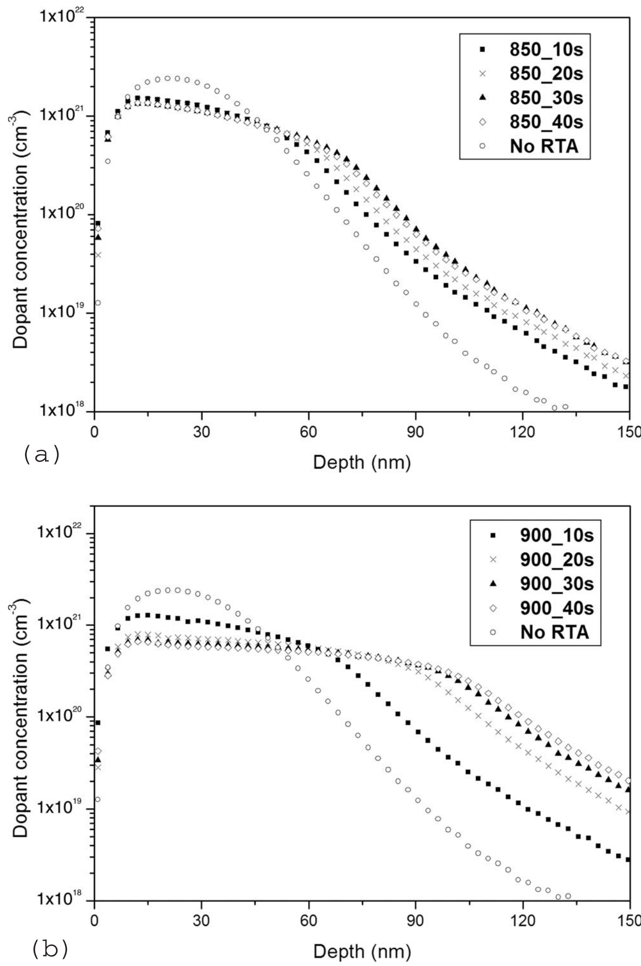

FIG. 2. SIMS results for RTA temperatures of (a) 850 °C and (b) 900 °C at varied RTA times.

shown in Fig. 1. Regular step structures were formed as the surface normal with a small offset angle α of 2.88° from [111] toward the $[\bar{2}11]$ direction.[20] The vicinal angle was obtained from the result of STM, and the value of the small offset angle α was 2.88° from the surface normal [111] direction. These vicinal Si(111) samples were implanted with P^+ ions with an energy of 20 keV and the dose of 1.0×10^{16} atoms/cm^2. The projected range of low-energy implantation was 28 nm. The RTA temperature was fixed at 850 and 900 °C, which were close to the optimal RTA condition.[10,12] The RTA process of these samples was carried out at the temperatures of 850 and 900 °C for 10, 20, 30, and 40 s in a N_2 gas environment.

The SHG experimental setup was the same as previously described.[10] Briefly, the RA-SHG measurement was performed using a *Q*-switched neodymium-doped yttrium aluminum garnet laser with 6 ns pulses at the wavelength of 1064 nm and 20 Hz repetition rate. With the *s*-polarized beam irradiated on the samples with an incident angle of 45°, the *s*-polarized SHG intensity was measured by a photomultiplier tube with a gated integrator. The SS-SHG intensity was recorded while the samples were rotated stepwise around their normal to vary the azimuthal angle.

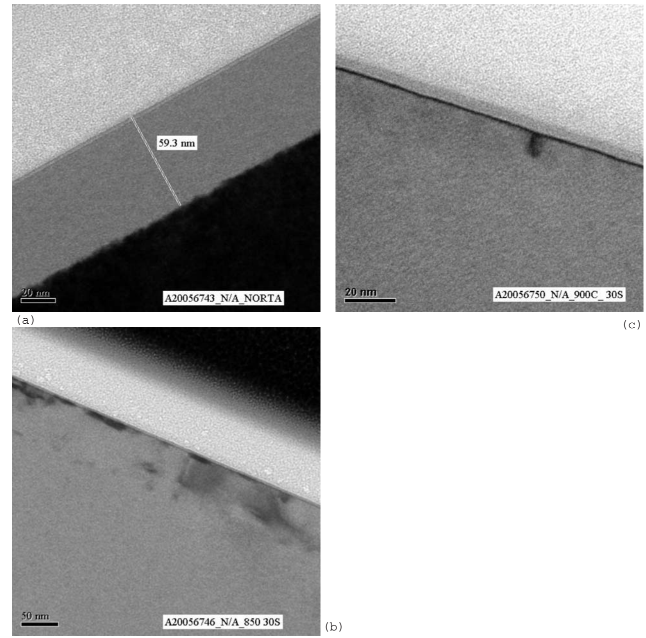

FIG. 3. TEM images of implanted Si(111) (a) without RTA and with RTA temperatures of (b) 850 °C and (c) 900 °C at RTA time of 30 s.

IV. RESULTS AND DISCUSSIONS

The distributions of dopant atoms at the annealing temperatures of 850 and 900 °C were obtained by SIMS and are shown in Figs. 2(a) and 2(b). (The diffusion coefficient of P in silicon is an exponential function of temperature, and its values are 8.19×10^{-17} and 4.28×10^{-16} cm^2/s for 850 and 900 °C, respectively.[21]) From Fig. 3(a), the amorphous (α)/crystalline (c) interface was 59.3 nm below the surface of the sample without the RTA process. At the RTA temperature of 850 °C, there were two sections of dopant redistribution separated by the α/c interface in the SIMS results, but this phenomenon was not obvious at the RTA temperature of 900 °C. Sadana *et al.* observed that the P atoms in the amorphous region do not redistribute on subsequent annealing, whereas the P atoms below the α/c interface diffuse rapidly into the silicon substrate.[22] Furthermore, they also found that the P atoms appear to be pinned near the surface region on subsequent annealing at ~850 °C, whereas the deeper parts

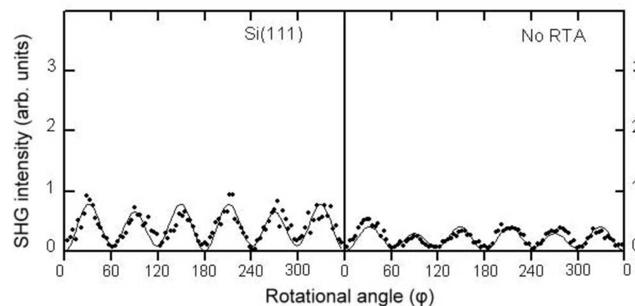

FIG. 4. SS-SHG results of Si reference substrate and implanted vicinal Si without the RTA process.

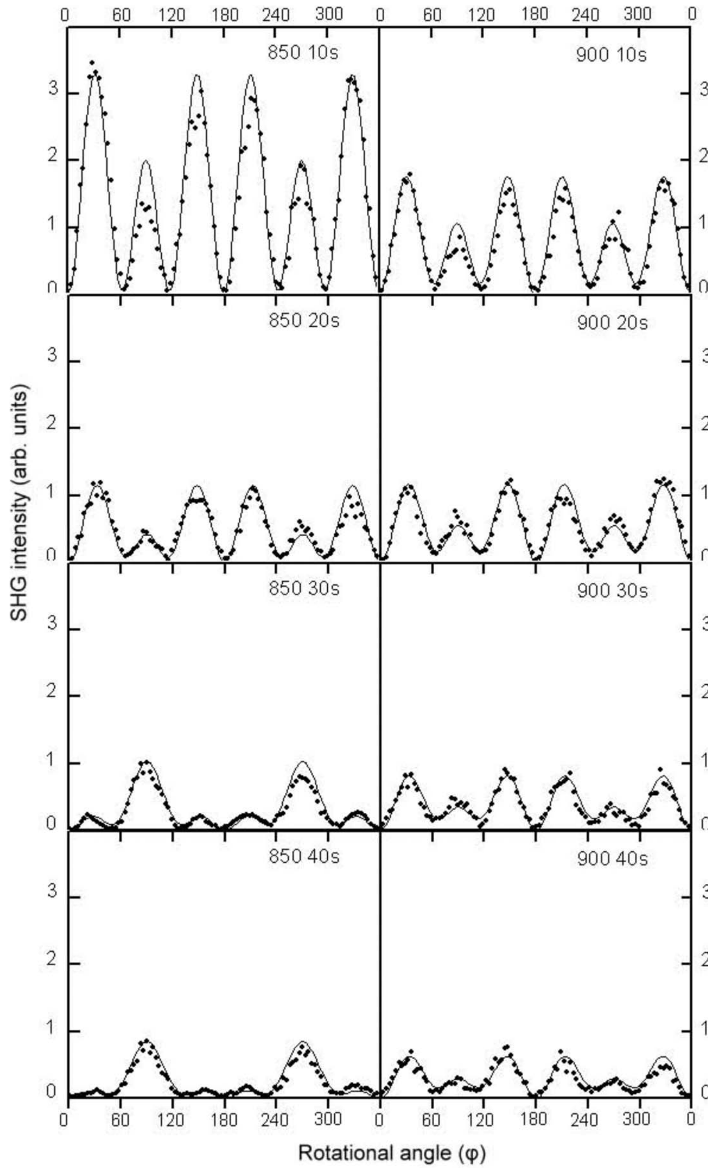

FIG. 5. SS-SHG results for the RTA temperatures of 850 and 900 °C with the RTA times of 10, 20, 30, and 40 s. The solid line is plotted by the fitting parameters listed in Table I.

showed pronounced diffusion effects. At higher annealing temperature (950 °C), the difference in the redistribution behavior of P atoms near the surface and deeper regions was no longer evident, and both regions showed normal diffusion effects. Our SIMS results agree with their work and the above summary is presented to illustrate the results in the SS-SHG analysis.

The SS-SHG results of the Si reference substrate (Si reference) and implanted vicinal Si without the RTA process (no RTA) are shown in Figs. 4(a) and 4(b), respectively. The SS-SHG results for the RTA temperatures of 850 and 900 °C with the RTA time of 10–40 s are exhibited in Fig. 5. The solid line was plotted by the results of the simulation of Eq. (2), which were fitted from the results of SS-SHG data. All fitting parameters are listed in Table I.

The SS-SHG intensity of implanted Si without the RTA process was less than that of the Si reference. It is reasonable that the damage caused by implantation will weaken the C_{3V} symmetry of the Si surface. The enhancement of RSHG intensity from implanted vicinal Si(111) is analyzed from the a_3 ratio of implanted Si(111) to Si reference substrate. From the theoretical analysis previously discussed,[11] the a_3 ratio could be described as

$$\frac{|a_3^T|}{|a_{3,\mathrm{Si}}|} \propto \frac{|I^T|^{1/2}}{|I_{\mathrm{Si}}|^{1/2}} \propto \frac{\int \chi_{ijk}^{(2),P} D_T(z)\exp[-\alpha(2\hbar\omega,z)z]\exp[-2\alpha(\hbar\omega,z)z]dz + \alpha^{-1}(2\hbar\omega,z)k\chi_{eff}^{Q}}{\alpha_0^{-1}(2\hbar\omega)k\chi_{eff}^{Q}}, \tag{3}$$

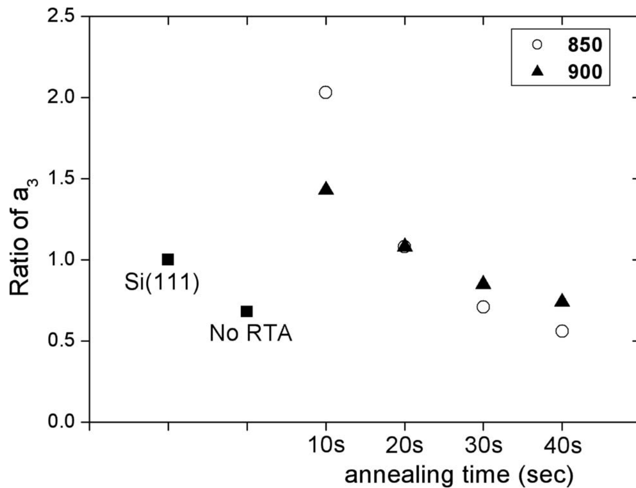

FIG. 6. a_3 ratio of implanted vicinal Si(111) to Si(111) substrate at RTA temperatures of 850 and 900 °C with RTA times of 10–40 s.

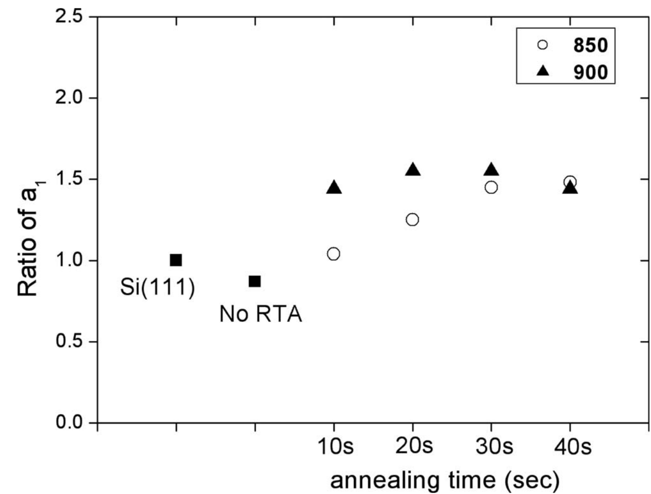

FIG. 7. a_1 ratio of implanted vicinal Si(111) to Si(111) substrate at RTA temperatures of 850 and 900 °C with RTA times of 10–40 s.

where the contribution of the surface dipoles from the steps of the vicinal Si surface $[\chi^{(2)}_{step}]$ is excluded since the symmetry of $\chi^{(2)}_{step}$ is C_{1V} symmetry. In the statement of Eq. (3), the ratio is strongly dependent on the dopant distribution (D_T), which is decided by the factor of RTA time at the situation of fixed RTA temperature and exhibited in SIMS profiles. The values of the a_3 ratio decrease as RTA time increases since the dopant density near the surface region reduces as the dopant atoms diffuse in the Si substrate. Figure 6 indicates that as RTA time increases, the a_3 ratio at the RTA temperature of 850 °C has a sharper decrease than that at the temperature of 900 °C. Surveying the SIMS results, the dopant density near the surface has only a slight variation at the RTA temperature of 850 °C. That is, the dopant density near the surface does not decrease with the diffusion effect. From the TEM images shown in Figs. 3(b) and 3(c), the precipitation of P atoms is more obvious at the RTA temperature of 850 °C. Nobili *et al.* found that when the solid solubility of P atoms in silicon is exceeded, the precipitation will occur.[23] Precipitation may contain many thousands of dopant atoms, and the size distribution of precipitates is related to the initial degree of supersaturation above solid solubility and thermal treatment given to the sample. Under different thermal treatments, more precipitation occurs at lower annealing temperature due to the lower solid solubility for high dopant dose herein, and this effect will weaken the residual electrical dipole formed in the suitable crystal site. Therefore, the sharper decrease of the a_3 ratio at the RTA temperature of 850 °C arises from the poor C_{3V} symmetry at the surface and is beyond the behavior of the dopant diffusion. These analyses are an illustration to explain the distinct changes of the a_3 value at different annealing temperatures of 850 and 900 °C. Thus the theoretical analysis in Eq. (3) is only suitable to explain the diffusion behavior without precipitation.

The relation of the a_1 ratio ($a_1/a_{1,\mathrm{Si\ substrate}}$) and the RTA time is shown in Fig. 7. The value of the a_1 ratio at the no RTA condition is less than unity. The ion implantation process leads to damage in the step structure of the vicinal Si/SiO_2 interface. Therefore, the net Si-O orientation normal to the steps is weakened. At the RTA temperature of 900 °C, the value of the a_1 ratio remains nearly constant and is larger than unity. The trend of the a_1 ratio at the RTA temperature of 850 °C grows from a value less than unity at the no RTA condition to a value that is the same as that in the RTA temperature of 900 °C. In the studies of Lüpke *et al.*,[13] the values of a_1 at different annealing temperatures were nearly equal to the value of the Si reference. Though the thickness of the native oxide layer in the implanted Si surface was more than that in the Si reference, the SHG field induced from the Si-O bondings on the steps would not increase with the oxide thickness since there was no more than one or two Si-O bondings per Si atom at the steps.[19] For the implanted vicinal Si(111) case, except for the RSHG contribution of the net Si-O orientation normal to the steps, there should be the residual electrical dipoles contributed to the RSHG intensity with mirror symmetry due to the morphological structure of the vicinal surface. These results lead to the enhancement in the value of a_1 and they correspond to the reconstruction condition of the vicinal surface. The growth of the a_1 ratio is interpreted to indicate that the activation energy at 850 °C is not enough to activate P atoms and the reconstruction of the implanted surface needs more annealing time at low activation energy. In the studies of Emmerichs *et al.*,[12] the a_1 component was strongly related to the relative atomic populations on the terraces and steps, and the oscillator strength would be influenced by the localization of the states. A proper annealing process caused a lower defect density on the step structure and more dangling bonds located on the step. Accordingly, the reconstruction of steps does not complete when there is not enough RTA time since the precipitation of P atoms happens in the RTA temperature of 850 °C.

The mechanism of the phase difference ψ_1 was determined by different chemically specific resonance energies at the step and terrace atom bonding sites.[24,25] The structural and chemical transition in the interfacial region from crystalline Si to amorphous SiO_2 is influenced by the crystal face

and thermal treatment of the oxide. The phase difference ψ_1 also has a large variation at the RTA temperature of 850 °C and RTA time of 30 s. Since the recrystallization rate and the solubility rate are lower at 850 °C, the reconstruction situation near the surface was completed until the RTA time of 30 s and was influenced by the precipitation of P atoms. The results agreed with the results of Emmerichs *et al.*[12] that the phase change is caused by the shift of resonance energy, which is dependent on the atomic structure on the steps.

The extended research in implanted Si using the RA-SHG method deeply analyzes the behaviors of the dopant diffusion by considering the precipitation of P atoms for a varied RTA process. The step structure of the vicinal Si is destroyed by ion implantation and its reconstruction is observed by the parts in mirror symmetry in the SS-SHG results. The uses of the vicinal Si surface and ion implantation give an improved diagnosis for the surface restructuring using the RA-SHG method. The step-induced onefold symmetry components of the RA-SHG response will distinguish the SHG contribution from the bulklike surface region layer. The variation in the value of a_1 reveals the reconstruction condition of the vicinal surface and the effect of RTA on the implanted Si surface.

V. CONCLUSION

The analysis of the SS-SHG intensity in implanted vicinal Si(111) presents many types of information, including the behavior of the dopant diffusion, recrystallization, and surface reconstruction. Although RSHG contributions from the surface and bulk are inseparable, the phenomena of the impurities diffusing into the bulk from the surface region are surveyed by a series of the RA-SHG experiments with varying RTA time and analyzed through the established theoretical method. The variation in the anisotropic contribution of C_{3V} symmetry reveals the behaviors of the dopant diffusion and the precipitation through different RTA processes, and these results illustrate the dependence on the RTA temperature and time. The step structure of the vicinal Si surface presents a chance to observe the reconstruction of the implanted surface and the role of impurities in the RTA process. The enhancement of the value of a_1 for the implanted vicinal Si(111) after the RTA process is originated from P atoms participating in the reconstruction process on the disorder surface and the residual electrical dipoles provide the contribution of C_{1V} symmetry according to the step structure in the vicinal surface. The SS-SHG measurement has been shown to be a sensitive and powerful tool for analyzing the surface reconstruction of the implanted vicinal Si(111).

ACKNOWLEDGMENTS

The authors would like to thank the National Science Council (NSC) of the Republic of China (Taiwan) for financially supporting this research under Contracts No. NSC 94-2112-M-415-006 and No. NSC 95-2112-M-415-002. K. M. Hung at the National Kaohsiung University of Applied Science is thanked for his helpful discussions. F. K. Men at National Chung Chang University is also appreciated for his assistance in STM analyses.

*kuanglo@mail.ncyu.edu.tw

[1] H. W. K. Tom, T. F. Heinz, and Y. R. Shen, Phys. Rev. Lett. **51**, 1983 (1983).
[2] C. V. Shank, R. Yen, and C. Hirlimann, Phys. Rev. Lett. **51**, 900 (1983).
[3] T. A. Driscoll and D. Guidotti, Phys. Rev. B **28**, 1171 (1983).
[4] D. Guidotti, T. A. Driscoll, and H. J. Gerritsen, Solid State Commun. **46**, 337 (1983).
[5] G. Lüpke, Surf. Sci. Rep. **35**, 75 (1999).
[6] V. Privitera, Curr. Opin. Solid State Mater. Sci. **6**, 55 (2002).
[7] R. J. Timans, W. Lerch, J. Niess, S. Paul, N. Acharya, and Z. Nenyei, 11th IEEE International Conference on Advanced Thermal Processing of Semiconductors-RTP 2003, 17 (2003).
[8] T. E. Seidel, D. J. Lischner, S. Pai, R. V. Knoell, D. M. Maher, and D. C. Jacobson, Nucl. Instrum. Methods Phys. Res. B **7-8**, 251 (1985).
[9] K. Y. Lo, Y. L. Wang, and J. D. Jin, Thin Solid Films **420-421**, 345 (2002).
[10] K. Y. Lo, J. Phys. D **38**, 3926 (2005).
[11] S. V. Govorkov, V. I. Emel'yanov, N. I. Koroteev, G. I. Petrov, I. L. Shumay, and V. V. Yakovlev, J. Opt. Soc. Am. B **6**, 1117 (1989).
[12] U. Emmerichs, C. Meyer, H. J. Bakker, H. Kurz, C. H. Bjorkman, C. E. Shearon, Jr., Y. Ma, T. Yasuda, Z. Jing, G. Lucovsky, and J. L. Whitten, Phys. Rev. B **50**, 5506 (1994).
[13] G. Lüpke, D. J. Bottomley, and H. M. van Driel, Phys. Rev. B **47**, 10389 (1993).
[14] C. W. van Hasselt, M. A. Verheijen, and T. Rasing, Phys. Rev. B **42**, 9263 (1990).
[15] Z. Jing, G. Lucovsky, and J. L. Whitten, Phys. Rev. B **49**, 14003 (1994).
[16] J. E. Sipe, V. Mizrahi, and G. I. Stegeman, Phys. Rev. B **35**, 9091 (1987).
[17] G. E. Jellison, S. P. Withrow, J. W. McCamy, J. D. Budai, D. Lubben, and M. J. Godbole, Phys. Rev. B **52**, 14607 (1995).
[18] G. E. Jellison, F. A. Modine, C. W. White, R. F. Wood, and R. T. Young, Phys. Rev. Lett. **46**, 1414 (1981).
[19] G. Lüpke, C. Meyer, U. Emmerichs, F. Wolter, and H. Kurz, Phys. Rev. B **50**, 17292 (1994).
[20] J. L. Lin, D. Y. Petrovykh, J. Viernow, F. K. Men, D. J. Seo, and F. J. Himpsel, J. Appl. Phys. **84**, 255 (1998).
[21] J. Pelleg and B. M. Ditchek, J. Appl. Phys. **73**, 699 (1992).
[22] D. K. Sadana, J. Wawhburn, and C. W. Magee, J. Appl. Phys. **54**, 3479 (1983).
[23] D. Nobili, A. Armigliato, M. Finetti, and S. Solmi, J. Appl. Phys. **53**, 1484 (1982).
[24] G. Lucovsky, A. Banerjee, H. Niimi, K. Koh, B. Hinds, C. Meyer, G. Luèpke, and H. Kurz, Appl. Surf. Sci. **117-118**, 202 (1997).
[25] Z. Jing, G. Lucovsky, and J. L. Whitten, Phys. Rev. B **49**, 14003 (1994).